Theoretical and Applied Genetics (2022) 135:527–535
https://doi.org/10.1007/s00122-021-03981-1

ORIGINAL ARTICLE

Fine mapping of the tiller inhibition gene *TIN4* contributing to ideal plant architecture in common wheat

Zhiqiang Wang[2] · Fangkun Wu[2] · Xudong Chen[2] · Wanlin Zhou[2] · Haoran Shi[2] · Yu Lin[2] · Shuai Hou[2] · Shifan Yu[2] · Hong Zhou[2] · Caixia Li[2] · Yaxi Liu[1,2]

Received: 9 September 2021 / Accepted: 19 October 2021 / Published online: 30 October 2021

Abstract

Key message **A tiller inhibition gene, *TIN4*, was mapped to an approximately 311 kb genomic interval on chromosome arm 2DL of wheat.**

Abstract The tiller is one of the key components of plant morphological architecture and a central agronomic trait affecting spike number in wheat. Low tiller number has been proposed as a major component of crop ideotypes for high yield potential. In this study, we characterized the development of tillering in near-isogenic lines (NIL7A and NIL7B), indicating that the TIN4 gene inhibited the growth of tillering buds and negatively regulated tiller number. Low-tillering was controlled by a single gene (TIN4) located on chromosome 2DL by genetic analysis and bulked segregant RNA-seq analysis. A total of 17 new polymorphic markers were developed in this study, and 61 recombinants were identified in the secondary F2 population containing 4,266 individuals. TIN4 was finally mapped on a 0.35 cM interval, co-segregated with molecular marker M380, within a 311 kb genomic interval of the wheat cultivar Chinese Spring reference genome sequence that contained twelve predicted genes. Yield experiments showed that the yield of low-tillering lines was higher than that of high-tillering lines at a higher density. Overall, this study provides a foundation for the construction of a low-tillering ideotype for improving wheat yield and further cloning TIN4 by map-based cloning approach.

Introduction

Branching is a common phenomenon in plant growth and development. Branches develop from axillary buds and determine plant architecture with high plasticity (Evers et al. 2011). In forestry, less branched or branchless plants form straight and sturdy main trunks owing to reduced resource

Communicated by Takao Komatsuda.

Zhiqiang Wang and Fangkun Wu contributed equally to this work.

✉ Yaxi Liu
liuyaxi@sicau.edu.cn

Zhiqiang Wang
frank.wang1991@hotmail.com

Fangkun Wu
1508479549@qq.com

Xudong Chen
1017246587@qq.com

Wanlin Zhou
1591736727@qq.com

Haoran Shi
542561234@qq.com

Yu Lin
646083078@qq.com

Shuai Hou
1912676042@qq.com

Shifan Yu
1608231625@qq.com

Hong Zhou
zhoubiu@qq.com

Caixia Li
493338068@qq.com

[1] State Key Laboratory of Crop Gene Exploration and Utilization in Southwest China, Wenjiang, Chengdu 611130, China

[2] Triticeae Research Institute, Sichuan Agricultural University, Wenjiang, Chengdu 611130, China

investment in branching, a feature that is conducive to transporting wood to mills for processing into various products (Rönnqvist 2003). In horticultural plants, such as kiwifruit vines (Cieslak et al. 2011) and apple trees (Lauri et al. 2008), more branches mean increased light and nutrient absorption areas, allowing maximum exploitation of external resources and thus, higher fruiting ability.

Tillers are special branches that arise from axillary buds at the basal nodes in gramineous plants, and is a pivotal agronomic trait determining spike number per plant and affecting crop yield (Wang et al. 2018). However, excessive numbers of tillers per plant can lead to reduced yield when they absorb excessive water and nutrients to enhance biomass but lower the proportion of productive spikes (Donald 1968; Kebrom et al. 2012). Compared with wild species, cultivated crops usually exhibit low tillering. The best-known example is maize, which usually has a single stem, without tillering. Maize was domesticated from teosinte, a highly branched plant. The *TB1* played a critical role in the domestication of maize; it inhibits the growth of axillary branches and promotes the formation of female inflorescence (Hubbard et al. 2002). Reduced tiller number has been used to increase yield in rice. The super rice cultivar (cv.) Yongyou12 and related genotypes are the beneficiaries of optimized expression of *IPA1* that confers an ideal plant architecture that generates high yield (Zhang et al. 2017). *IPA1* and *TB1* suppress tillering and allow the ears of individual plants to obtain a higher nutrient supply, thereby forming larger spikes/ears and heavier kernels, ensuring an increase in crop yield.

Similarly, in wheat, more than half a century ago, Donald (1968) proposed a wheat ideotype for high grain yield. It consisted of one or few tillers, short plant height, large spikes, and erect leaves. Identification and characterization of tillering genes/quantitative trait loci (QTL) are essential preconditions for designing tillering to improve wheat. To date, several single genes (*tin1*, *tin2*, *tin3*, and *ftin*) inhibiting tillering have been identified in wheat (Kuraparthy et al. 2007; Peng et al. 1998; Spielmeyer and Richards 2004; Zhang et al. 2013). Further, numerous QTL affecting tiller number have been reported, such as *QTn.ipk-1B*, *QTn.ocs.5A.1*, and *QTn.mst-6B* (Huang et al. 2003; Kato et al. 2000; Liu et al. 2018, 2020; Nasseer et al. 2016; Ren et al. 2018).

In previous studies, we identified a major QTL on the chromosome arm 2DL (*Qltn.sicau-2D*, herein named *TIN4*) that significantly reduced tiller number in different genetic backgrounds (Wang et al. 2016). Near-isogenic lines (NILs) targeting this gene were developed based on molecular marker-assisted selection (Wang et al. 2019). In the present study, we characterized the *TIN4* to suppress tillering bud growth and negatively regulate tiller number, and fine mapped *TIN4* to a 0.35 cM genetic interval corresponding to a 311 kb genomic interval of the wheat cultivar Chinese Spring genome (IWGSC_Refseq v1.0).

Materials and methods

Plant materials

Common wheat H461, a progeny from the cross between SW94-30,921/Yiyuan2, harbors allele *TIN4* that confers a significantly reduced tiller number (Wang et al. 2016). The NILs NIL7A and NIL7B were developed from a segregating family in the recombinant inbred line population developed from a cross between H461 and a wheat cultivar chuannong16 (Wang et al. 2019). To fine-map the *TIN4*, a population of 4,266 F_2 individuals was generated from a cross between the high-tillering isoline NIL7A and the low-tillering isoline NIL7B. Tiller numbers of the population were evaluated at growth stage (GS) 85 (Zadoks et al. 1974) (see Fig. 1 for outline of growth stages in wheat). F_2 population and F_3 families of the recombinants were planted in the field at Sichuan Agricultural University, Wenjiang District, Chengdu, China, under natural conditions with conventional management. F_3 families were single-seed planted in 2 rows 1.5 m, with 10 cm between plants within a row and rows spaced 30 cm apart. Twenty plants of each F_3 family were evaluated.

The effects of *TIN4* on yield were assessed by testing two pairs of NILs (NIL7A/B and NIL11A/B) (Zhou et al. 2020) at two field trials, one at Chongzhou (2017−2018, 103°38'E, 30°32'N) and the other at Wenjiang (2019−2020, 103°51'E, 30°43'N). Five seeding densities (40, 158, 277, 395, and 514 seeds/m^2) with three replicates were used in a randomized block design for each trial. Each plot consisted of 10 rows of 1.5 m each, with rows spaced 30 cm apart. Field management as described above without supplementary irrigation, the max/min temperature and rainfall during growing season are shown in Fig S1. The wheat spikes in each plot were hand-harvested at GS87 and measured total weight of grains after drying to constant weight under natural conditions.

Morphological and histochemical analysis

The plant and tiller morphologies from GS12 to GS15 were recorded and examined using a camera and an SMZ745T light stereomicroscope (Nikon, Japan). For histochemical analysis, shoot bases were collected after 1-WAP (week after planting) and 2-WAP, and then fixed in formaldehyde–acetic acid–alcohol solution at 4 °C for 48 h. The method used for sample preparation by paraffin sectioning was modified from that described by Duan et al. (2019); tissues were unstained and then examined using a BX51 fluorescence microscope (Olympus, Tokyo, Japan).

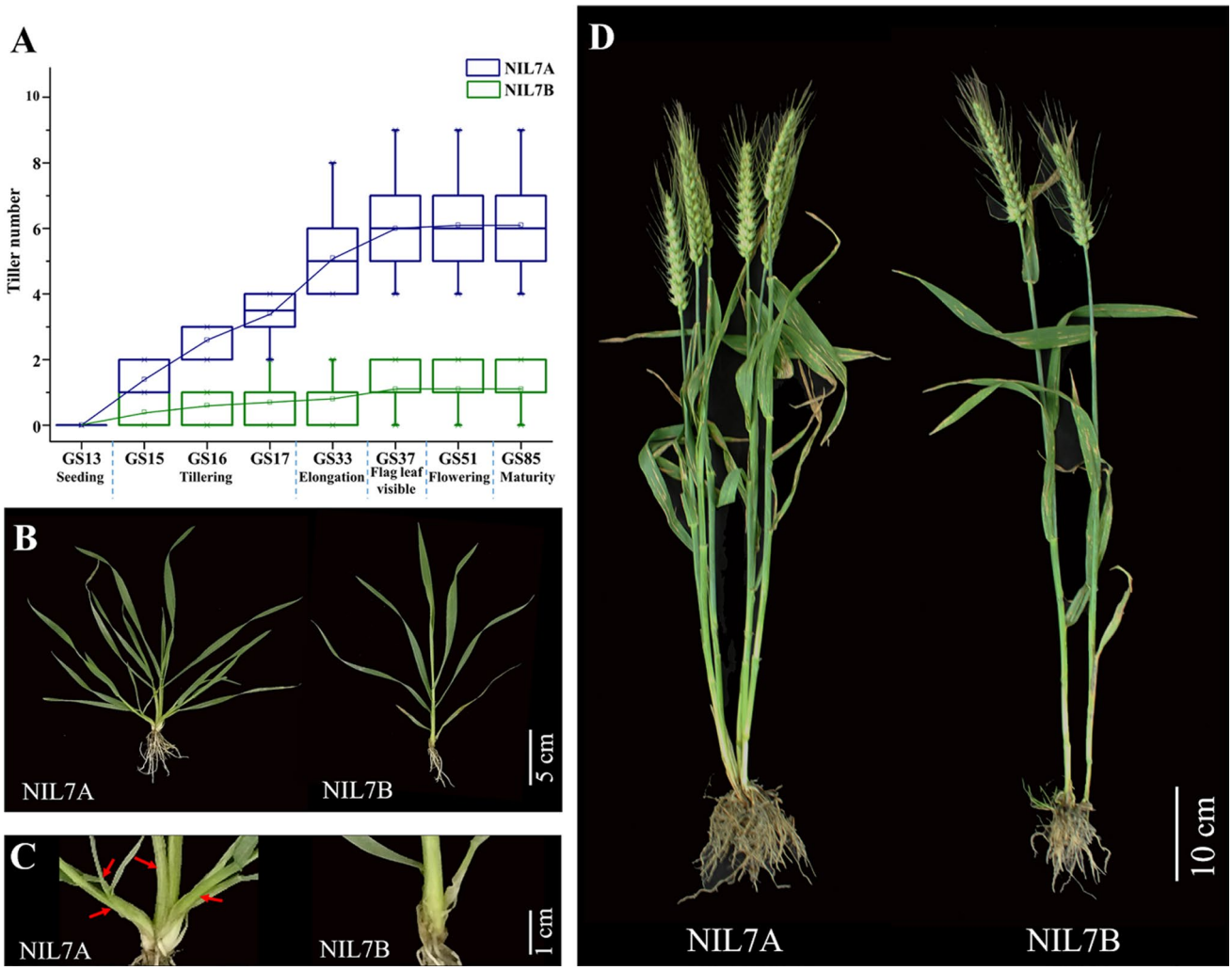

Fig. 1 Phenotypic characterization of near-isogenic lines NIL7A and NIL7B. **a** Tiller numbers of NIL7A and NIL7B from GS 13 to GS 85. **b** Tiller phenotypes of NIL7A and NIL7B at GS 17. **c** Enlarged images of shoot bases. Red arrows indicate tillers. **d** Tillering phenotypes of NIL7A and NIL7B at GS 85

Bulked segregant RNA-seq (BSR-seq) analysis

For RNA sequencing (RNA-seq), 40 low-tillering plants (Bulk-low) and 40 high-tillering plants (Bulk-high) were selected from an F_2 population (238 individuals) of the NIL7A/NIL7B cross. Approximately the same size flag leaf segments were samples from each individual at GS 37 and pooled separately based on phenotype. RNA was extracted using the Total RNA purification kit according to the user's manual (LC-Bio, CA, USA), and DNA was removed using DNase I.

cDNA libraries were constructed following the manufacturer's instructions (Vazyme Biotech, China) and sequenced using a HiSeq2500 system (Biomarker, China). Raw sequence data were checked for quality using the NGS QC Toolkit (Patel and Jain 2012) and then aligned to the wheat reference genome (IWGSC_Refseq v1.0, https://urgi.versailles.inra.fr/download/iwgsc/) using BWA (Li 2012). The multiple mapping and PCR-duplication reads were filtered using SAMtools (Li et al. 2009) and Picard MarkDuplicates (http://broadinstitute.github.io/picard/). Single nucleotide polymorphisms (SNPs) were identified using BCFtools (Narasimhan et al. 2016), and a minimum cutoff of ten reads was retained using Perl script. The SNP-index values of the two bulks were calculated using MutMap (Abe et al. 2012) with the following formula: $\text{index}^{\text{NIL7A}} = N_{\text{NIL7A}}/(N_{\text{ref}} + N_{\text{NIL7A}})$, where N represents the number of accumulated reads with the corresponding genotypes. The ΔSNP-index for each SNP was calculated using the formula $\Delta\text{SNP-index} = \text{index}^{\text{NIL7A}} - \text{index}^{\text{NIL7B}}$. The ΔSNP-index values were raised to the power of 4 ($\Delta\text{SNP-index}^4$) to decrease the noise caused by small variations in the estimations. The data were fitted using a Loess curve, with the fitted values as the median of the 50 upstream and downstream SNPs.

High ΔSNP-index^4 values were used to identify the candidate region containing *TIN4*. The datasets generated during the current study are available at the National Center for Biotechnology Information (NCBI) SRA repository under accession number PRJNA705399.

DNA extraction and marker development

Genomic DNA was extracted from the leaves of 30-day-old plants following the cetyl trimethyl ammonium bromide (CTAB) method (Murray and Thompson 1980), and the concentration was adjusted to about 100 ng/µl.

The candidate region containing *TIN4* located in a previous study (Wang et al. 2016) was targeted to develop markers based on SNPs, insertion–deletions (Indels), and simple sequence repeats (SSRs) between the isolines NIL7A and NIL7B. SSR markers were designed with SSRMMD (Gou et al. 2020) based on the sequences in the candidate region of the wheat reference genome. Polymerase chain reaction (PCR) was performed using routine procedures, and PCR products were separated by 6% non-denaturing polyacrylamide gel electrophoresis. The NIL7A and NIL7B RNA-seq data (Wang et al. 2019) were used for calling SNPs and Indels. Based on the SNPs, high-resolution melting (HRM) and Kompetitive allele-specific PCR (KASP) markers were also developed and tested for polymorphisms between NIL7A and NIL7B following previously described methods (Tan et al. 2017; Wang et al. 2019). The new polymorphic markers detected between NIL7A and NIL7B are listed in Table S1.

Molecular mapping of *TIN4*

Linkage analysis and genetic map construction were performed using JoinMap 4.0 (Van Ooijen 2006) with a 3.0 LOD threshold. A small population of 238 F_2 individuals from the NIL7A/NIL7B cross and newly developed markers were initially utilized to map *TIN4*. The flanking markers were subsequently used to screen for recombinants in an F_2 population of 4266 individuals. A high-density genetic map, based on the recombinants, was constructed for the targeted interval.

Statistical analysis

Data analyses were performed and graphs were produced using the Origin v9.0 program (OriginLab Corporation, USA). Differences between groups were considered significant at $P < 0.05$ based on Student's *t* tests. A chi-square test was performed to test the phenotypic data for determining if tillering was controlled by a single gene.

Results

Phenotypic characterization of NILs

Comparison of tiller number between NIL7A and NIL7B at different growth stages, a significant difference was detected between NIL7A (1.50 ± 0.50) and NIL7B (0.4 ± 0.49) at GS 15, with increasing phenotypic divergence from GS 15 to GS 85 (Fig. 1). Finally, the tiller number of NIL7B was found significantly decreased by 85% compared with NIL7A (Fig. 1a). Histological analysis revealed no significant difference between the isolines in either tiller bud initiation or the number of tiller buds at 1 and 2 weeks after sowing (Fig. S2). Microscopic observation showed that the number of tillering buds was consistent during GS 12 to 13, while significant differences in tillering bud development were observed between near-isogenic lines during GS 14 to 15 (Fig. 2, Fig. S3). Specifically, the growth from tillering buds in the low-tillering NIL7B was inhibited, and there was no progress to secondary tillering buds, thus leading to significantly reduced tiller numbers. In addition, the thousand kernel weight of NIL7B was significantly higher than that of NIL7A (Fig. S4), but there was no significant difference between the lines in plant height, flag leaf length, flag leaf width, spike length, or flowering time (Fig. S5).

The genetic background of NIL7A and NIL7B was highly similar, only 1346 (~2.7%) markers were polymorphic between NIL7A and NIL7B using the wheat 55 K SNP Array (Wang et al. 2019). A small F_2 population consisting of 238 individuals from the NIL7A/NIL7B cross was phenotyped for tiller number. The numbers of low-tillering and high-tillering individuals fitted a 3:1 ratio (173:65; $\chi^2 = 0.56 < \chi^2_{0.05,\,1} = 3.84$), indicating that the *TIN4* phenotype was conferred by a single dominant gene.

BSR-seq analysis and molecular mapping of *TIN4*

After quality control, Bulk-low and Bulk-high generated 60,881,504 and 67,713,424 reads by RNA-seq, respectively (Table S2). 67,490 credible SNPs were identified in Bulk-high and 68,815 credible SNPs were identified in Bulk-low by software analysis. A total of 51,069 SNPs were common between the two bulks and were used to further calculate the SNP index (Fig. 3a). BSR-Seq analysis based on the ΔSNP-index^4 was used to measure allelic segregation and to identify markers linked with the *TIN4* based on SNPs between the two bulks. One single significant peak for ΔSNP-index^4 was located in a region of approximately 3.17 Mb on chromosome arm 2DL, and this reconfirmed that the *TIN4* phenotype was controlled by a single dominant gene (Fig. 3b, c).

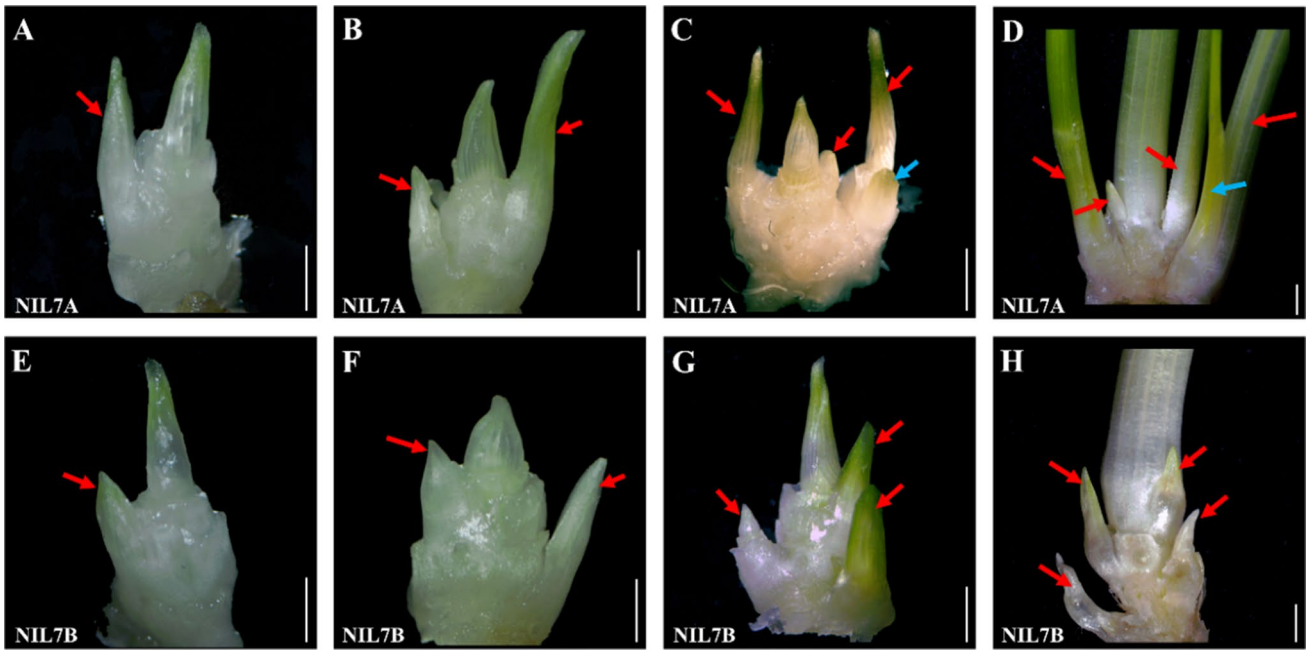

Fig. 2 Tillering buds or tillers of NIL7A and NIL7B at GS 12 **(a, e)**, GS 13 **(b, f)**, GS 14 **(C, G)**, and GS 15 **(D, H)**. Red arrows indicate the primary tillering buds or tillers; blue arrows indicate the secondary tillering buds or tillers; Bar, 2 mm

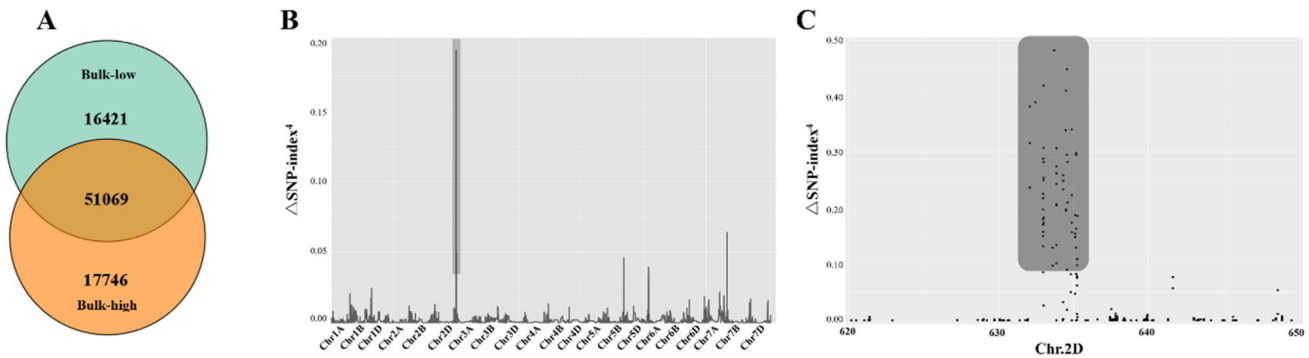

Fig. 3 BSR-seq analysis. **a** The number of SNPs identified in the Bulk-low and Bulk-high. **b** Identification of the genomic region contributing to low-tillering number by BSR-Seq analysis. Black lines show the Loess fit curve calculated from the △SNP-index4. **c** △SNP-index^4 scores of the candidate region on chromosome 2D

Fine mapping of the *TIN4*

Eleven polymorphic markers were developed around the candidate region and used to genotype the 238 F_2 individuals derived from NIL7A/NIL7B. A linkage map with 4.9 cM was constructed and mapped *TIN4* to a 1.73 cM interval between markers M3 and N82 (Fig. 4a). The flanking markers were then used to screen recombinants from a large F_2 population of 4266 individuals, and 61 recombinants were identified. To further narrow down the genetic interval of the *TIN4* locus, six newly polymorphic markers (M44, M52, M207, M251, M380, and M323) within the interval were developed and used to construct a high-density genetic map (Fig. 4b). The tiller number of F_2 and $F_{2:3}$ families in homozygous recombinants were evaluated for classifying the *TIN4* genotype (Fig. S6; Fig. 4c). Finally, *TIN4* was identified to co-segregate with marker M380, and was placed within a 0.35 cM genetic interval delimited by markers M251 and M323 (Fig. 4b).

Referred to the reference genome of the wheat cultivar Chinese Spring (IWGSC_Refseq v1.0), this interval covered a 311 kb sequence of Chinese Spring 2DL. Twelve high confidence predicted genes were annotated according to IWGSC_Refseq v1.1 (Fig. 4d, Table 1). Identified the orthologues of these twelve genes in rice and *Arabidopsis*, none of were orthologues to the known tillering or branching gene,

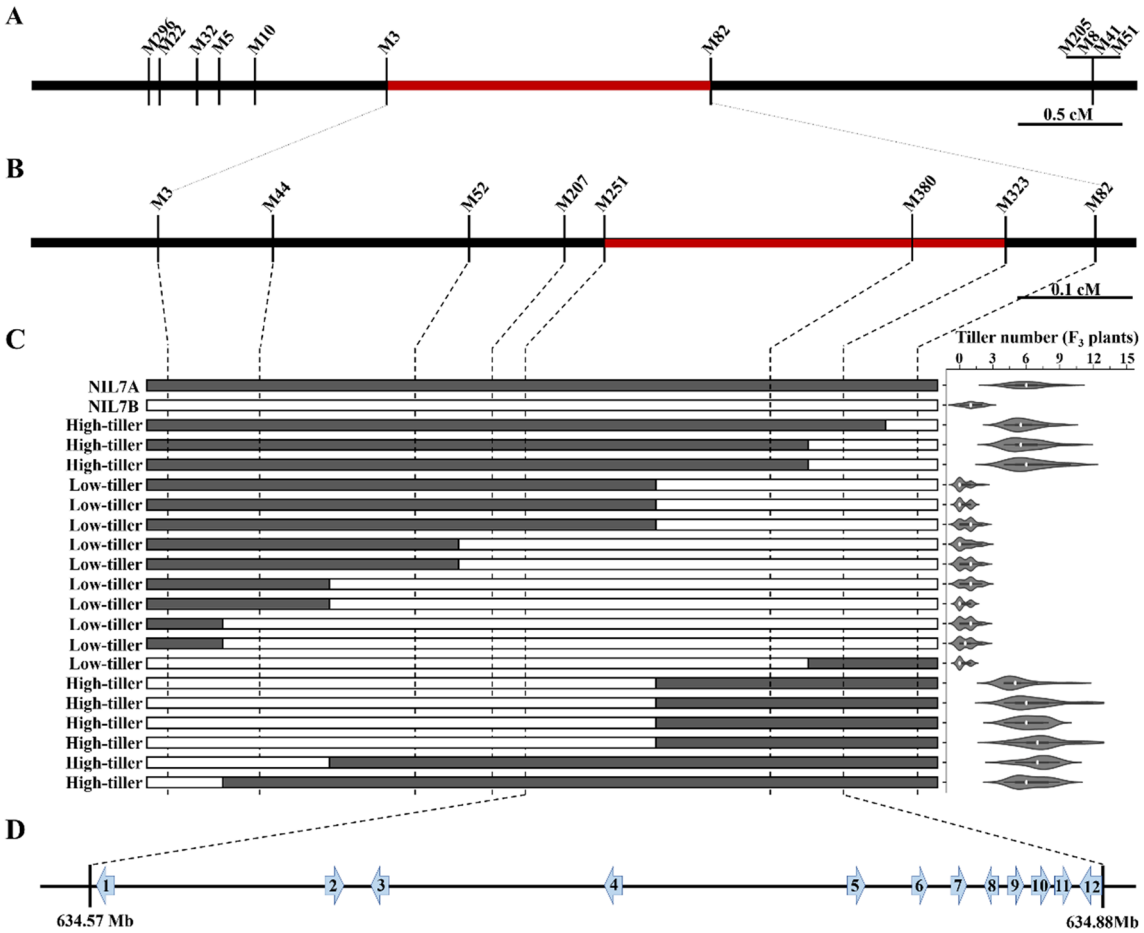

Fig. 4 Mapping of the *TIN4*. **a** Mapping of *TIN4* based on a segregating F_2 population (NIL7A x NIL7B) of 238 individuals. **b** Fine mapping of *TIN4* based on an F_2 population of 4,266 individuals. **c** Genotypes and phenotypes of homozygous recombinants identified with markers surrounding the *TIN4*. The gray regions represent alleles from NIL7A and the white ones for alleles from NIL7B. The average tiller number to each of these recombinant lines ($F_{2:3}$) and parents were provided on the right hand side of the diagram. **d** Physical map of the target region in the reference genome of wheat based on IWGSC RefSeq v1.0

Table 1 Annotations of predicted genes in the genomic region of *TIN4*

No	Predicted gene ID	Annotation
1	*TraesCS2D02G563200*	Dof zinc finger protein
2	*TraesCS2D02G563300*	–
3	*TraesCS2D02G563400*	Dof zinc finger protein
4	*TraesCS2D02G563500*	–
5	*TraesCS2D02G563600*	NADPH-protochlorophyllide oxidoreductase
6	*TraesCS2D02G563700*	NADPH-protochlorophyllide oxidoreductase
7	*TraesCS2D02G563800*	–
8	*TraesCS2D02G563900*	Cytochrome P450, family 96 protein
9	*TraesCS2D02G564000*	*N*-acetylglucosaminylphosphatidylinositol deacetylase
10	*TraesCS2D02G564100*	Sugar/polyol transporter
11	*TraesCS2D02G564200*	Clathrin light chain
12	*TraesCS2D02G564300*	–

contained two encoded dof zinc finger proteins, two encoded NADPH-protochlorophyllide oxidoreductases, one encoded members of cytochrome P450 protein family, one encoded N-acetylglucosaminylphosphatidylinositol deacetylase, one encoded sugar/polyol transporter, one encoded clathrin light chain and four encoded unknown protein.

Yield response to seeding density and tillering capacity

Two pairs of NILs were assessed for yield under five seeding densities. Variance analysis revealed that genotype and seeding density had significant effects on yield, and interaction between genotypes and seeding density was also significant effect on yield (Table S3). With increasing seeding densities from 40 to 514 seeds/m^{-2}, grain yields increased and then decreased in both trials. The optimal seeding densities for the two trials were 277 and 395 seeds/m^2, respectively (Fig. 5). As expected, grain yield in the low-tillering lines (NIL7B and NIL11B) with the *TIN4* allele were lower than that of the high-tillering lines (NIL7A and NIL11A) at lower seeding densities. Conversely, yields of the low-tillering lines were higher than those of the high-tillering lines at higher seeding densities. Importantly, the maximum yield of the low-tillering lines was 2.26%–13.33% higher than that of the high-tillering lines (Table S4).

Discussion

Tillers are special branch organs determining the morphological architecture and grain yield in wheat. Tillering development consists of three main stages: (a) the formation of axillary meristem, (b) further development until tillering bud formation, and (c) growth of the tillering bud into a tiller (Hussien et al. 2014). Genes can regulate the tiller number by influencing axillary meristem formation. For example, in rice, the absence of MOC1 protein in *moc1* mutant blocks the initiation of the axillary meristem, thereby reducing the tiller number (Li et al. 2003). Some genes such as *D3* and *D10* in rice and *TaD27*, *tin1*, and *dmc* in wheat (An et al. 2019; Arite et al. 2007; Ishikawa et al. 2005; Kebrom et al. 2012; Zhao et al. 2020) inhibit the elongation and growth of tillering buds and negatively regulate tiller number. Compared with NIL7A, tillering buds in NIL7B were inhibited and could not grow into tillers, further restricting the formation of secondary tillers. These observations suggested that *TIN4* inhibit the growth of tillering buds and negatively regulate tiller number.

In wheat, four tillering inhibition genes (*tin1*, *tin2*, *tin3*, and *ftin*) have been reported. Spielmeyer and Richards (Spielmeyer and Richards 2004) mapped a tiller inhibition gene (*tin1*) on the short arm of chromosome 1A, and mapped on a 0.08 cM region spanning 101 kb on the physical map of Chinese Spring (Hyles et al. 2017). The *tin2* was mapped on chromosome 2A (Peng et al. 1998). Meanwhile, *tin3* was identified in diploid wheat and mapped to a 4.1 cM region of chromosome 3A between the markers XSTS-TR3L6 and XSTS-TR3L4 (Kuraparthy et al. 2008). The fourth gene *ftin* was most likely located on the wheat chromosomal deletion bin 0.86 ~ 1.00 of chromosome arm 1AS (Zhang et al. 2013). In addition, numerous QTL for tiller number in wheat have been reported (Li et al. 2010; Liu et al. 2014, 2018; Nasseer et al. 2016; Ren et al. 2018). However, only a few explained high phenotypic variation, and even fewer major QTL for tiller number were identified among multiple environments. In our previous study, we reported a tillering inhibition gene (*TIN4*) mapped on chromosome arm 2DL and explained up to 19.1% of the phenotypic variance, and further developed NILs for *TIN4* (Wang et al. 2016, 2019). In this study, we confirmed that *TIN4* was located on 2DL by BSR-Seq analysis and finally mapped *TIN4* to a 311 kb genomic region of

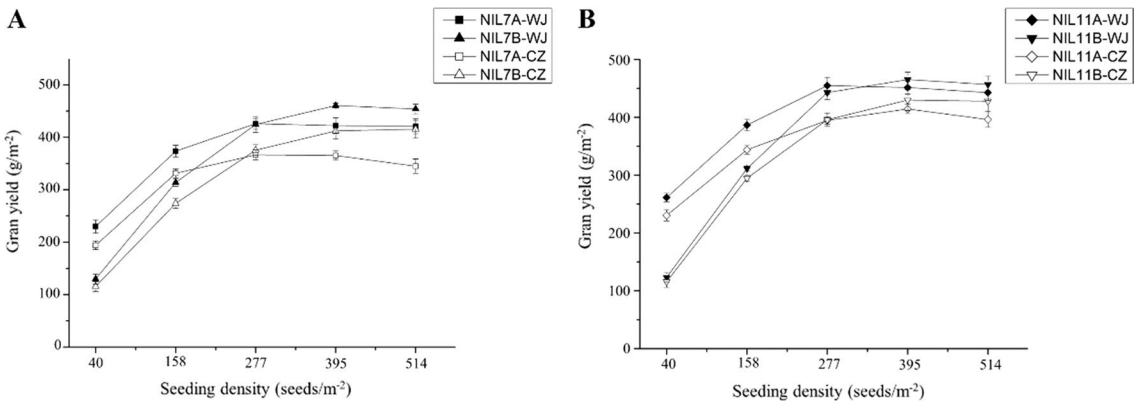

Fig. 5 Effects of seeding density on yield. **a** Difference in grain yield between NIL7A and NIL7B across the two trials. **b** Difference in grain yield between NIL11A and NIL11B across the two trials. WJ: Wenjaing, CZ: Chongzhou. Error bars represent the SD

the reference genome. Twelve high-confidence genes were identified and none of were orthologues to the known tillering, implying the *TIN4* may be a new tillering regulation gene in wheat. In summary, this study is helpful to further clone *TIN4* and reveal the mechanism of tillering formation in wheat.

TIN4 regulates tiller number so effectively that it can be used to design a wheat ideotype that was proposed half a century ago (Donald 1968), but has not been successfully implemented in wheat production. The main reason was that adverse traits such as unproductive tillers, low grain weight, and excessive vegetative growth were associated with the low-tillering trait (Liu et al. 2020; Naruoka et al. 2011; Yan 2017; Zhang et al. 2013). The *ftin* allele delays the growth and development of tillers, resulting in the formation of unproductive tillers and fewer fertile tillers (Zhang et al. 2013). In this study, the *TIN4* significantly reduced tiller number, without any unproductive tillers (Fig. 1). This highlights *TIN4* as a new gene regulating tillering, opening up possibilities for applications in breeding by molecular design to increase wheat yield.

The *TIN4* has the potential to increase yield requiring seeding densities above 277 seeds/m^2. Mitchell (Mitchell et al. 2013) proposed that tiller inhibition genes provide the potential to increase production per unit area. This would be achieved by fewer competing tillering meristems, making more assimilates available to the spikes, resulting in larger spikes and higher kernel weight. Low-tillering wheat is also beneficial in terms of a more uniform spike canopy and overall spike maturity that is more convenient for harvesting using a combined harvester. In this study, low-tillering lines carrying *TIN4* allele exhibited higher yields than high-tillering lines at higher seeding density (395 seeds/m^2), increased yield can compensate for increased seed costs. Overall, *TIN4* can achieve optimal yield at higher seeding density, and incorporating *TIN4* into wheat is expected to develop wheat varieties with high yield potential.

Supplementary Information The online version contains supplementary material available at https://doi.org/10.1007/s00122-021-03981-1.

Acknowledgements This study was supported by the National Natural Science Foundation of China (31771794), and the Key Research and Development Program of Sichuan Province (2021YFN0034 and 21ZDYF3575).

Author contributions ZQW and FKW drafted and revised the manuscript, and mainly responsible for data analysis; XDC, WLZ, YL, SH, SFY and HZ performed the experiments; HRS and CXL participated in data analysis; YXL conceived and coordinated the project, and revised the manuscript; and all authors read and approved the final manuscript for publication.

Data Availability The sequencing datasets in this study can be accessed at the National Center for Biotechnology Information (NCBI) SRA repository under accession number PRJNA705399 and PRJNA657689.

Declarations

Conflict of interest All authors declare that there is no conflict of interest.

Ethical Approval The authors declare that the experiments comply with the current laws of the country in which they were performed.

References

Abe A, Kosugi S, Yoshida K, Natsume S, Takagi H, Kanzaki H, Matsumura H, Yoshida K, Mitsuoka C, Tamiru M (2012) Genome sequencing reveals agronomically important loci in rice using MutMap. Nat Biotechnol 30:174–178

An J, Niu H, Ni Y, Jiang Y, Zheng Y, He R, Li J, Jiao Z, Zhang J, Li H (2019) The miRNA–mRNA networks involving abnormal energy and hormone metabolisms restrict tillering in a wheat mutant dmc. Int J Mol Sci 20:4586

Arite T, Iwata H, Ohshima K, Maekawa M, Nakajima M, Kojima M, Sakakibara H, Kyozuka J (2007) DWARF10, an RMS1/MAX4/DAD1 ortholog, controls lateral bud outgrowth in rice. Plant J 51:1019–1029

Cieslak M, Seleznyova AN, Hanan J (2011) A functional–structural kiwifruit vine model integrating architecture, carbon dynamics and effects of the environment. Ann Bot 107:747–764

Donald CM (1968) The breeding of crop ideotypes. Euphytica 17:385–403

Duan E, Wang Y, Li X, Lin Q, Zhang T, Wang Y, Zhou C, Zhang H, Jiang L, Wang J (2019) OsSHI1 regulates plant architecture through modulating the transcriptional activity of IPA1 in rice. Plant Cell 31:1026–1042

Evers JB, van der Krol AR, Vos J, Struik PC (2011) Understanding shoot branching by modelling form and function. Trends Plant Sci 16:464–467

Gou X, Shi H, Yu S, Wang Z, Li C, Liu S, Ma J, Chen G, Liu T, Liu Y (2020) SSRMMD: a rapid and accurate algorithm for mining SSR feature loci and candidate polymorphic SSRs based on assembled sequences. Front Genet 11:706

Huang X, Cöster H, Ganal M, Röder M (2003) Advanced backcross QTL analysis for the identification of quantitative trait loci alleles from wild relatives of wheat (Triticum aestivum L.). Theor Appl Genet 106:1379–1389

Hubbard L, McSteen P, Doebley J, Hake S (2002) Expression patterns and mutant phenotype of teosinte branched1 correlate with growth suppression in maize and teosinte. Genetics 162:1927–1935

Hussien A, Tavakol E, Horner DS, Muñoz-Amatriaín M, Muehlbauer GJ, Rossini L (2014) Genetics of tillering in rice and barley. Plant Genome. https://doi.org/10.3835/plantgenome2013.10.0032

Hyles J, Vautrin S, Pettolino F, MacMillan C, Stachurski Z, Breen J, Berges H, Wicker T, Spielmeyer W (2017) Repeat-length variation in a wheat cellulose synthase-like gene is associated with altered tiller number and stem cell wall composition. J Exp Bot 68:1519–1529

Ishikawa S, Maekawa M, Arite T, Onishi K, Takamure I, Kyozuka J (2005) Suppression of tiller bud activity in tillering dwarf mutants of rice. Plant Cell Physiol 46:79–86

Kato K, Miura H, Sawada S (2000) Mapping QTLs controlling grain yield and its components on chromosome 5A of wheat. Theor Appl Genet 101:1114–1121

Kebrom TH, Chandler PM, Swain SM, King RW, Richards RA, Spielmeyer W (2012) Inhibition of tiller bud outgrowth in the tin

mutant of wheat is associated with precocious internode development. Plant Physiol 160:308–318
Kuraparthy V, Sood S, Dhaliwal H, Chhuneja P, Gill BS (2007) Identification and mapping of a tiller inhibition gene (tin3) in wheat. Theor Appl Genet 114:285–294
Kuraparthy V, Sood S, Gill BS (2008) Genomic targeting and mapping of tiller inhibition gene (tin3) of wheat using ESTs and synteny with rice. Funct Integr Genomics 8:33–42
Lauri P-E, Costes E, Regnard J-L, Brun L, Simon S, Monney P, Sinoquet H (2008) Does knowledge on fruit tree architecture and its implications for orchard management improve horticultural sustainability? An overview of recent advances in the apple. I Int Symp Hortic Europe 817:243–250
Li H (2012) Exploring single-sample SNP and INDEL calling with whole-genome de novo assembly. Bioinformatics 28:1838–1844
Li X, Qian Q, Fu Z, Wang Y, Xiong G, Zeng D, Wang X, Liu X, Teng S, Hiroshi F (2003) Control of tillering in rice. Nature 422:618–621
Li H, Handsaker B, Wysoker A, Fennell T, Ruan J, Homer N, Marth G, Abecasis G, Durbin R (2009) The sequence alignment/map format and SAMtools. Bioinformatics 25:2078–2079
Li Z, Peng T, Xie Q, Han S, Tian J (2010) Mapping of QTL for tiller number at different stages of growth in wheat using double haploid and immortalized F 2 populations. J Genet 89:409
Liu G, Jia L, Lu L, Qin D, Zhang J, Guan P, Ni Z, Yao Y, Sun Q, Peng H (2014) Mapping QTLs of yield-related traits using RIL population derived from common wheat and Tibetan semi-wild wheat. Theor Appl Genet 127:2415–2432
Liu J, Luo W, Qin N, Ding P, Zhang H, Yang C, Mu Y, Tang H, Liu Y, Li W (2018) A 55 K SNP array-based genetic map and its utilization in QTL mapping for productive tiller number in common wheat. Theor Appl Genet 131:2439–2450
Liu J, Tang H, Qu X, Liu H, Li C, Tu Y, Li S, Habib A, Mu Y, Dai S (2020) A novel, major, and validated QTL for the effective tiller number located on chromosome arm 1BL in bread wheat. Plant Mol Biol 104:173–185
Mitchell J, Rebetzke G, Chapman S, Fukai S (2013) Evaluation of reduced-tillering (tin) wheat lines in managed, terminal water deficit environments. J Exp Bot 64:3439–3451
Murray M, Thompson WF (1980) Rapid isolation of high molecular weight plant DNA. Nucleic Acids Res 8:4321–4326
Narasimhan V, Danecek P, Scally A, Xue Y, Tyler-Smith C, Durbin R (2016) BCFtools/RoH: a hidden Markov model approach for detecting autozygosity from next-generation sequencing data. Bioinformatics 32:1749–1751
Naruoka Y, Talbert L, Lanning S, Blake N, Martin J, Sherman J (2011) Identification of quantitative trait loci for productive tiller number and its relationship to agronomic traits in spring wheat. Theor Appl Genet 123:1043
Nasseer A, Martin J, Heo H, Blake N, Sherman J, Pumphrey M, Kephart K, Lanning S, Naruoka Y, Talbert L (2016) Impact of a quantitative trait locus for tiller number on plasticity of agronomic traits in spring wheat. Crop Sci 56:595–602
Van Ooijen J (2006) JoinMap® 4, Software for the calculation of genetic linkage maps in experimental populations. Kyazma BV, Wageningen 33
Patel RK, Jain M (2012) NGS QC Toolkit: a toolkit for quality control of next generation sequencing data. PLoS ONE 7:e30619
Peng Z, Yen C, Yang J (1998) Genetic control of oligo-culms character in common wheat. Wheat Inf Serv 86:19–24
Ren T, Hu Y, Tang Y, Li C, Yan B, Ren Z, Tan F, Tang Z, Fu S, Li Z (2018) Utilization of a Wheat55K SNP array for mapping of major QTL for temporal expression of the tiller number. Front Plant Sci 9:333
Rönnqvist M (2003) Optimization in forestry. Math Program 97:267–284
Spielmeyer W, Richards R (2004) Comparative mapping of wheat chromosome 1AS which contains the tiller inhibition gene (tin) with rice chromosome 5S. Theor Appl Genet 109:1303–1310
Tan C-T, Yu H, Yang Y, Xu X, Chen M, Rudd JC, Xue Q, Ibrahim AM, Garza L, Wang S (2017) Development and validation of KASP markers for the greenbug resistance gene Gb7 and the hessian fly resistance gene H32 in wheat. Theor Appl Genet 130:1867–1884
Wang Z, Liu Y, Shi H, Mo H, Wu F, Lin Y, Gao S, Wang J, Wei Y, Liu C (2016) Identification and validation of novel low-tiller number QTL in common wheat. Theor Appl Genet 129:603–612
Wang B, Smith SM, Li J (2018) Genetic regulation of shoot architecture. Annu Rev Plant Biol 69:437–468
Wang Z, Shi H, Yu S, Zhou W, Li J, Liu S, Deng M, Ma J, Wei Y, Zheng Y (2019) Comprehensive transcriptomics, proteomics, and metabolomics analyses of the mechanisms regulating tiller production in low-tillering wheat. Theor Appl Genet 132:2181–2193
Yan J (2017) A functional–structural kiwifruit vine model integrating architecture, carbon dynamics and effects of the environment. China Agriculture Press
Zadoks JC, Chang TT, Konzak CF (1974) A decimal code for the growth stages of cereals. Weed Res 14:415–421
Zhang J, Wu J, Liu W, Lu X, Yang X, Gao A, Li X, Lu Y, Li L (2013) Genetic mapping of a fertile tiller inhibition gene, ftin, in wheat. Mol Breeding 31:441–449
Zhang L, Yu H, Ma B, Liu G, Wang J, Wang J, Gao R, Li J, Liu J, Xu J (2017) A natural tandem array alleviates epigenetic repression of IPA1 and leads to superior yielding rice. Nat Commun 8:1–10
Zhao B, Wu TT, Ma SS, Jiang DJ, Bie XM, Sui N, Zhang XS, Wang F (2020) TaD27-B gene controls the tiller number in hexaploid wheat. Plant Biotechnol J 18:513–525
Zhou W, Shi H, Wang Z, Zhao Y, Gou X, Li C, Chen G, Liu S, Deng M, Ma J (2020) Identification of lncRNAs involved in wheat tillering development in two pairs of near-isogenic lines. Funct Integr Genomics 20:669–679